5th ECPMG Delft · 2024

Proceedings of the 5th ECPMG 2024
5th European Conference on Physical Modelling in Geotechnics
2-4 October 2024, Delft, the Netherlands

3D Experiments in bath: groundwater in geosynthetic-reinforced pile-supported embankments

Suzanne J.M. van Eekelen, Britt Wittekoek, Rob A. Zwaan,
Deltares, Delft, Netherlands, suzanne.vaneekelen@deltares.nl, britt.wittekoek@deltares.nl rob.zwaan@deltares.nl

Adam Bezuijen
Bezuijen Consult, Berkel en Rodenrijs, Netherlands, adambezuijen@bezuijenzonsult.nl

Alain Nancey
Solmax, Paris, France, anancey@solmax.com

ABSTRACT: This paper presents small-scale 3D experiments that investigate how groundwater affects the behaviour of geosynthetic-reinforced pile-supported (GRPS) embankments. To conduct these experiments, an existing test set-up was submerged in a bath.
The experiments showed that groundwater reduces the load that is exerted on the piles. This is primarily due to Archimedes' uplift forces, rather than a change in soil arching. The pile loading quickly recovers when the groundwater level decreases again. No significant correlation between groundwater level and geosynthetic reinforcement strains was observed.

1 GROUNDWATER IN EXPERIMENTS ON PILED EMBANKMENTS

This paper looks at the impact of fluctuating groundwater levels on the behaviour of geosynthetic-reinforced pile-supported (GRPS) embankments. Limited literature exists on the physical modelling of water in piled embankments. Song et al. (2018) and Wang et al. (2019) are two examples.

Song et al. (2018) conducted simple small-scale 2D trapdoor tests on saturated and unsaturated sand, without geosynthetic reinforcement (GR). First, they saturated the sand by immersing it in water and stirring it every hour for at least 48 hours. Subsequently, the saturated sand was placed into the model box, using a small shovel, aiming to prevent compaction and thereby minimizing the sand density.

Then, they lowered the water table in their tests by pumping water out of the box at the bottom. They measured the pressure on the trapdoor, leading to the conclusion that the soil arching increased with lowering groundwater level.

Wang et al. (2019) conducted full-scale 3D experiments that were much closer to real-world GRPS embankments. The 3.2 m high, well-compacted embankment consisted of different gravel layers. At the top, they placed five holes (50 mm diameter, 200 mm depth), along the longitudinal direction for water injection, simulating the infiltration of rain in a railway embankment. Eight actuators simulated train passages. Contrary to Song et al. (2018), Wang et al. (2019) showed an increase in soil arching with an increasing groundwater level; the dynamic soil stresses on the pile caps slightly increased as the groundwater level rose.

This paper presents experiments where the water level was increased and decreased from below. This matches the situation in typical road scenarios, where rainwater flows from the road surface into a ditch or infiltrates into the roadside verges. This indirectly leads to a rising groundwater level until the water has been drained, evaporates or has been pumped away.

2 SCALED EXPERIMENTS

Figure 1 shows the test setup (van Eekelen et al., 2012, 2024). A steel plate supports a sealed and soaked foam cushion, equipped with a drainage tap. Four PVC piles with a diameter of 0.1 m pass through the steel plate.

Two Geolon 100-50 woven geotextiles were attached to a stiff steel frame, perpendicular to and directly on top of each other. Their combined tensile strength was 100+50 = 150 kN/m and their combined tensile stiffness at 2% strain $J_{2\%}$ was 1200 kN/m and 1013 kN/m after 10 and 1000 hours loading, respectively.

A water cushion was used to apply an equally distributed surcharge load. A rubber sheet, lubricated with Vaseline minimised the wall-soil friction. The load distribution in the fill was measured using total pressure cells.

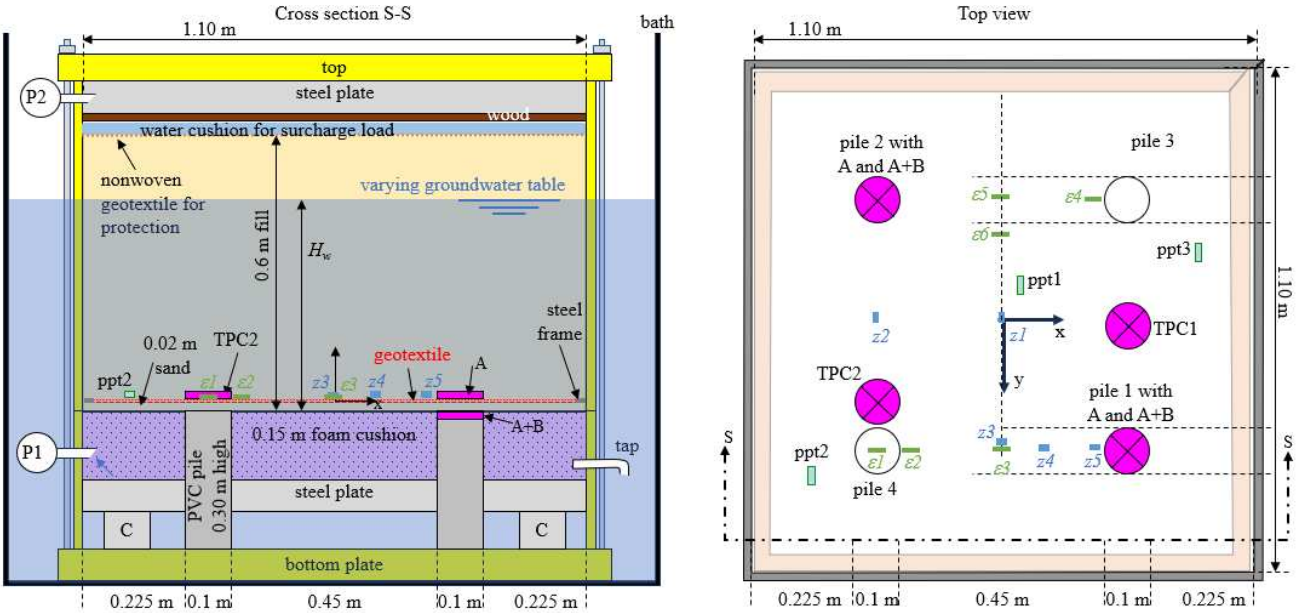

Figure 1. Test setup of the GRPS embankment in bath for inducing groundwater fluctuations within the fill. (van Eekelen et al. 2024). All transducers above the geotextile were installed directly on top of the geotextile.

The GR deflection (z1 to z5) was measured with a liquid levelling system comprising water pressure cells in tubes filled with water and connected to a reference box with water.

The GR strains ('ε'), were measured with bicycle brake cables. The twisted steel wire that runs through an outer sleeve, was pulled out by approximately 10 mm and attached to the geotextile. A displacement transducer registered the difference between the displacement of the twisted steel wire and the outer sleeve.

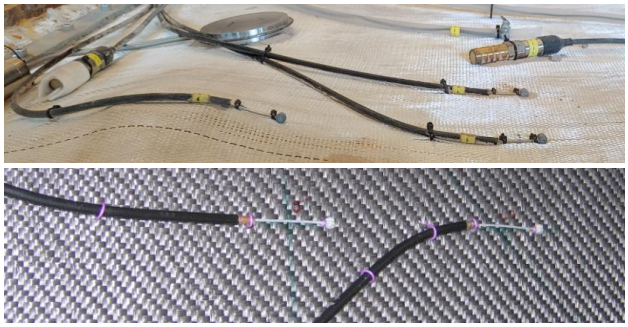

Figure 2. Strain cables. Above: current tests; below: Test TC2 of van Eekelen et al. 2012, with more connection points between strain cable and geotextile. Similar geotextiles were used.

A similar system to measure GR strains was applied in van Eekelen et al. (2012). However, back then, it was concluded that it is necessary to attach the cables to the geosynthetic with tie ribs at short distances. If the distances become too large, the cables tend to give too high strains (even larger than the rupture strain, without observing rupture upon excavation). However, even in that case the system still gives a qualitatively consistent picture of the strains that occur in the geosynthetic.

During the years, this finding was forgotten. Therefore, the distance between the tie ribs was relatively large, as shown in Figure 2. And indeed, several measured values were unrealistically large. However, similar to the results of van Eekelen et al. (2012), the system provided a consistent qualitative result, as discussed further in Section 4.2.

Two types of mixed demolition waste granulate were used; one with fine content (d/D = 0/31.5 mm) and one without fine content (d/D = 4/31.5 mm), where d and D are the lower and upper sieve sizes (NEN-EN13242, 2015).

Table 1 lists the fill details. The values of $\varphi'_{15\%}$ were obtained from four drained large-scale triaxial tests shown in Figure 3. Two triaxial tests per fill type were conducted; one on saturated fill and one on unsaturated (initial) fill material (approximately 5.4% of water).

Table 1. Test details of the three small-scale tests.

Test no.	1	2	3
Fill height above steel (m)	0.65	0.60	0.60
Limiting sieve sizes d/D (mm/mm)	4/31.5	0/31.5	4/31.5
Median particle size D_{50} (mm)	18.8	7.0	18.8
Unit weight dry fill γ_d (kN/m^3)	13.19	14.60	13.20
Unit weight saturated fill γ_s (kN/m^3)	18.11	19.00	18.12
Unit weight initial fill γ_i (kN/m^3)	13.90	15.39	13.91
Porosity n (V_{pores} / V_{total})	0.50	0.45	0.50
Friction angle unsaturated fill $\varphi'_{15\%}$ (°)	41.0	39.4	41.0
Friction angle saturated fill $\varphi'_{15\%}$ (°)	40.5	39.6	40.5

Figure 3. 0.45 m diameter drained triaxial tests on the fill

After the installation of the reinforcement, sensors and fill, the test box was closed and placed in the empty bath. Then, the subsoil support was removed by creating a vacuum in the foam cushion.

Subsequently, the bath was filled and emptied slowly (Figure 4), approximately one cycle in 1.5 days, to minimize the occurrence of air inclusions. Complete prevention of air inclusions was not anticipated, this was accepted as it aligns with real-world conditions.

Figure 4. The test setup in the bath, with the 0.205 m wide rubber duck highlighting the water level.

The testing box, designed and constructed in 2009, had several openings to allow cables and pipes to exit. These openings, located at the bottom of the box, proved to be sufficiently large and evenly distributed to facilitate the smooth passage of water from the bath into the test box.

The groundwater table on top of the geotextile, in the fill closely followed the water level in the bath. It could easily be monitored not only with the pore pressure transducers (ppts) in the fill, but also with the ppt in the foam cushion that was sucked vacuum at the bottom of the test box. Both corresponded with the measurements of the water level in the bath.

The groundwater table was then lowered again (in Tests 2 and 3 only). After that, the surcharge load was increased in steps. After each surcharge load step, a groundwater cycle was applied again. In Test 1, the phreatic line was kept constant.

3 CALCULATIONS

The three main European design methods for GRPS embankments are:

- The Concentric Arches model of van Eekelen et al. (2013, 2015, adopted in CUR226, 2016);
- The model of Zaeske (2001), adopted in EBGEO, (2011);
- The model of Hewlett and Randolph (1988) adopted in both the French ASIRI (2012) and the British Standard (BS8006, 2010).

The first calculation step of these models divides the vertical load into two parts (Figure 5). Part A (kN/pile) is directly transferred to the piles and is relatively large, due to soil arching. The residual load, 'B+C' (kN/pile) is supported by the subsurface between the piles.

The second calculation step determines the GR strain, which implicitly divides B+C further into B and C. In the current tests, the foam cushion underneath the GR was sucked vacuum, removing the subsoil support during the entire test, so that C = 0.

3.1 Input parameters

Figure 1 provides the geometry properties, and Table 1 lists the fill properties. The groundwater table H_w was derived from the measured pore pressures (ppt 1, 2 and 3). The weighted value of γ in equations (2) to (5) was derived from γ_d below groundwater level (combined with Archimedes' p_{uplift} for the grains) and γ_i (kN/m^3) above groundwater level. γ_i is the initial fill unit weight that includes the 5.4% moisture content of the sand above the phreatic line.

The wall-soil friction R was 20-25% of the total load and was derived by subtracting the measured total load (A+B+C) from the applied total load. The resulting R was subtracted from the surcharge load. There was no subsoil support, so the subgrade reaction k was 0 kN/m^3. The geotextile tensile stiffness $J_{2\%}$ was chosen in line with the test duration: $J_{2\%}$ = 1106 kN/m.

3.2 Water in the calculations

Archimedes' principle states that a body immersed in a fluid is subject to an upward force equal to the weight of the displaced fluid. Van Eekelen et al. (2024) explains how Archimedes' upward pressure (p_{uplift}) can be used to account for the water in the fill. The upward pressure is defined as:

$$p_{uplift} = (1\text{-}n) \cdot H_w \cdot \gamma_w \text{ (kPa)} \quad (1)$$

where n (-) is the porosity, H_w (m) is the ground-water table above the piles, and γ_w is the unit weight of water (9.81 kN/m^3).

p_{uplift} is integrated in the CA calculations by reducing the surcharge load p with p_{uplift}. This approach aligns Terzaghi's effective stress calculations. Van Eekelen et al., 2024 explains why using Archimedes is possible, and using the Terzaghi's effective stresses is not possible for models like the CA model (CUR226) and the EBGEO model.

The CA model uses the following equations:

$$A_{p>0} = \frac{\gamma H+p}{\gamma H} \cdot A_{p=0} \text{ and} \quad (2)$$

$$(B+C)_{p>0} = \frac{\gamma H+p}{\gamma H} \cdot (B+C)_{p=0} \quad (3)$$

In this study, groundwater is brought into these equations as follows:

$$A_{p>0} = \frac{\gamma H+p-p_{uplift}}{\gamma H} \cdot A_{p=0} \text{ and} \quad (4)$$

$$(B+C)_{p>0} = \frac{\gamma H+p-p_{uplift}}{\gamma H} \cdot (B+C)_{p=0} \quad (5)$$

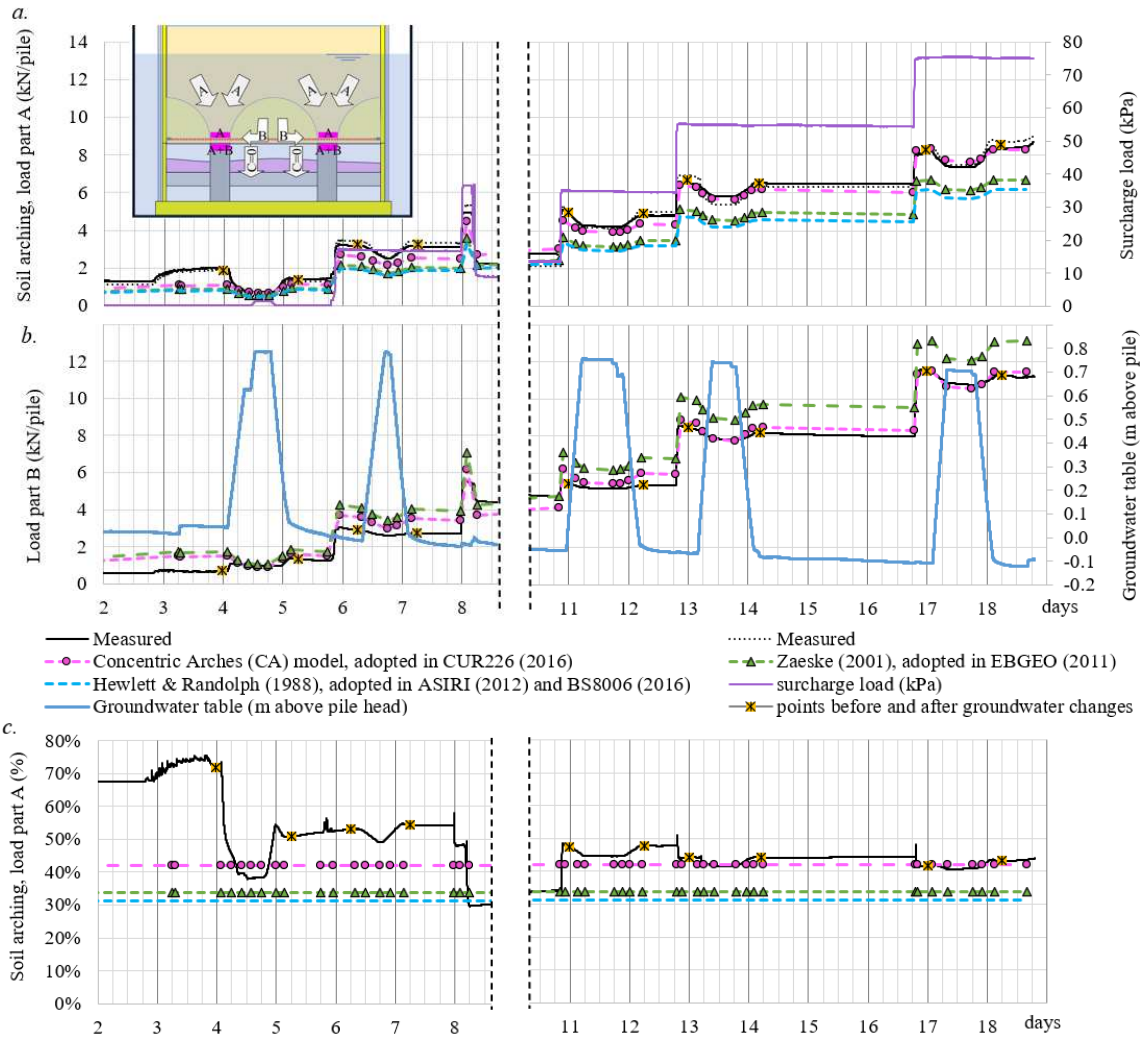

Figure 5. Comparison measured and calculated load distribution for Test 2. a. Soil arching (load part A). b. Load part B. c. Load part A in % of the total load. The 'measured' value of B was derived from the average measured values of A+B and A. p_{uplift} was included in all calculations by reducing surcharge load p with p_{uplift}. Between days 8 and 11, the surcharge load cushion leaked.

4 IMPACT OF GROUNDWATER

4.1 Impact groundwater on soil arching

Figure 5 compares the measured and calculated soil arching for Test 2. We observe the following:

A rising groundwater level results in a limited decrease in both A and B (kN/pile).

The reduction in load is primarily due to the uplift forces of Archimedes' principle. In other words, the decrease is a result of the decreasing load rather than a change in soil arching. This is evident in the close match between measurements and calculations. The calculations included the Archimedes uplift (a load reduction) but did not include a reduction in soil arching.

Figure 5c eliminates the influence of Archimedes' uplift, by showing the soil arching as a percentage of the total load (A% = A/(total load per unit) in kN/kN). This graph shows a slight decrease in A% due to groundwater, indicating that the soil arching experiences some reduction. We conclude that the decrease in A is not solely attributable to the Archimedes effect (the reduction in load), even though this remains the most significant mechanism at play.

The soil arching (A) almost immediately rebounds when the phreatic line decreases.

The soil arching changes less than ±3.5% due to the full groundwater cycles. The only exception is the first groundwater cycle, which decreases the arching by 26% (difference between A (kN/pile) before and after the full cycle). At that stage, the arching had not found its equilibrium yet.

The CA model matches the measurements better than the other two calculation models. Both EBGEO and Hewlett and Randolph (1988) underestimate the soil arching.

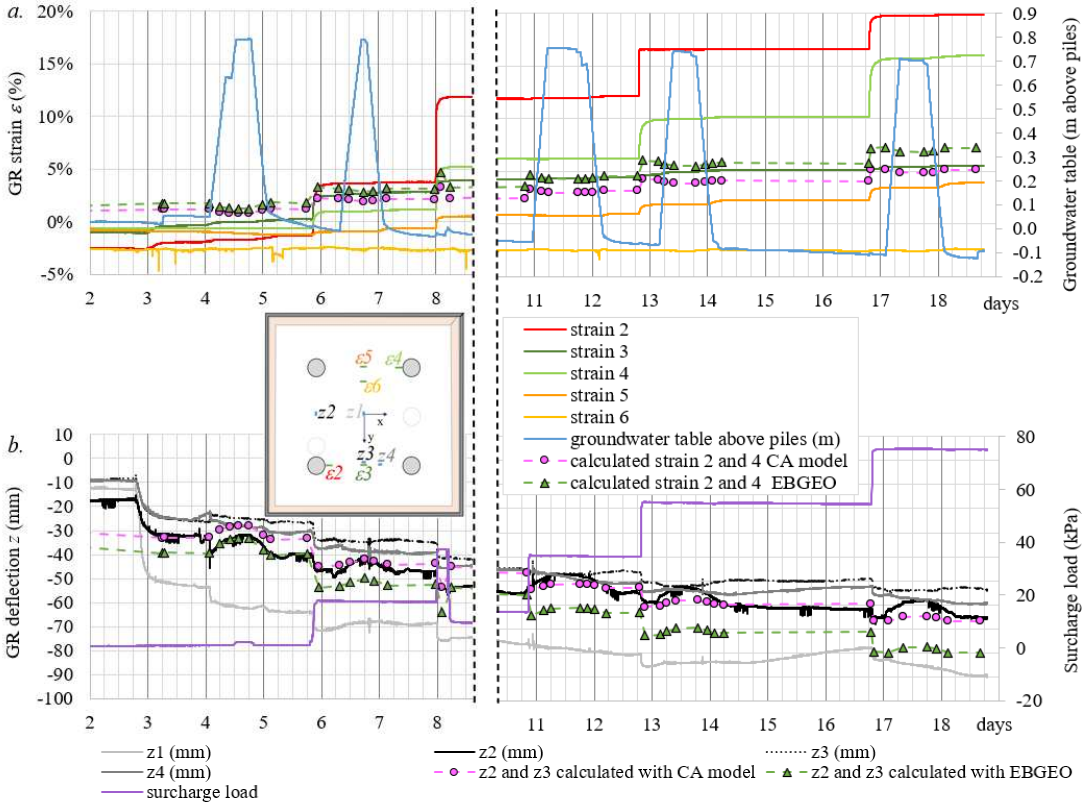

Figure 6. Measured and calculated deformations and strains. a. GR strains ε, and b. GR deflection z.

4.2 Impact of groundwater on GR strains

Section 2 described why the strain cables only provided a qualitative result. Nevertheless, the measurements appear qualitatively reliable, as shown in Figure 6a, and in further measurements presented in van Eekelen et al. (2024). This finding matches our expectations: the highest GR strains were measured in the strips between adjacent piles, with the strain increasing closer to the pile. Outside the GR strip between adjacent piles (ε6), we observe much lower strains, typically around zero.

The GR strains do not respond significantly to changes in groundwater level. This matches the findings of van Eekelen et al. (2023), who also found no convincing correlation between water and GR strain in field measurements. Temperature appeared to show a stronger correlation with the GR strain.

4.3 Impact of groundwater on settlements

Figure 6b compares the measured and calculated GR deflection at the midpoint between two piles. The CA model matches the measured deflection nicely. Some settlement transducers show heave due to rising groundwater, specifically sensor z2. The calculations also show this effect, although to a lesser extent.

5 FILL WITH FINES OR NO FINES

Van Eekelen et al. (2024) compare the measured and calculated results for all three tests, that include both types of fill. They show that all three tests respond similarly to groundwater rise: a reduction in load and GR deflection, with a quick rebound after the high-water period. The CA calculations match the impact of groundwater well, if the uplift forces are accounted for using Archimedes' principle, as described in Section 3.2.

6 CONCLUSIONS

Experiments were conducted to investigate the impact of groundwater in a GRPS embankment. To introduce the water into the fill, the test box was placed in a bath. The bath was slowly filled and emptied, resulting in a phreatic line that rose and lowered slowly. Openings located at the bottom of the test box facilitated the smooth passage of water from the bath into the test box and vice versa.

The following conclusions were drawn:

- Groundwater reduces the load due to uplift forces.
- The reduction of load part A, which expresses soil arching, is primarily caused by the uplift forces, but a rising groundwater level also leads to a slight change in soil arching.
- The soil arching immediately recovers when the groundwater level is lowered again.
- The CA model provides a closer match to the measurements than the other two considered calculation models (EBGEO and Hewlett and Randolph (1988)), both of which underestimate the soil arching.
- The response on groundwater rise is similar for both fill types, with and without fines.
- An increase of groundwater results in some heave of the GR, due to the uplift forces. This heave disappears upon lowering the groundwater again.
- The presented experiment did not reveal any significant response of GR strains to changes in groundwater. This is in line with the findings of van Eekelen et al. (2023), who observed a correlation between air temperature and GR strain, and not between the groundwater table and GR strain in the field.

ACKNOWLEDGEMENTS

The authors are grateful for the support of Solmax-TenCate, both financially and practically, and the support of the TKI-PPS funding of the Dutch Ministry of Economic Affairs.

REFERENCES

ASIRI (2013). *Recommendations for the design, construction and control of rigid inclusions ground improvements* (French version is of 2012).

Archimedes. (circa 250 BCE). Archimedes' Principle.

BS8006-1 (2010). Code of practice for strengthened/reinforced soils and other fills. British Standards Institution, UK.

CUR226 (2016). See Van Eekelen and Brugman (2016).

Hewlett, W.J. and Randolph, M.F. (1988). Analysis of piled embankments. Ground Eng. 21(3): 12-18.

NEN-EN 13242 (2015) *Hydraulic bound and unbound aggregates*.

Song, J., Chen, K., Li, P., Zhang, Y. and Sun, C. (2018). Soil arching in unsaturated soil with different water table. *Granular Matter*, 20: 78.

van Eekelen, S.J.M., Bezuijen, A., Lodder, H.J. and van Tol, A.F. (2012). Model experiments on piled embankments Part I. *Geotextiles and Geomembranes*, 32: 69-81.

van Eekelen, S.J.M., Bezuijen, A. van Tol, A.F., (2013). An analytical model for arching in piled embankments. *Geotextiles and Geomembranes* 39: 78-102.

van Eekelen, S.J.M., Bezuijen, A. and Van Tol, A.F. (2015). Validation of analytical models for the design of basal reinforced piled embankments. *Geotextiles and Geomembranes*, 43(1): 56 - 81.

van Eekelen, S.J.M. and Brugman, M.H.A., Eds. (2016). *Design Guideline Basal Reinforced Piled Embankments* (CUR226). CRC Press, Delft, Netherlands.

van Eekelen, S.J.M., Venmans, A.A.M., Bezuijen, A. and van Tol, A.F. (2020). Long term measurements in the Woerden geosynthetic-reinforced pile-supported embankment. *Geosynth. Int.,* 27(2): 142-156.

van Eekelen, S.J.M., Zwaan, R.A., Nancey, A., Hazenkamp, M. and Jung, Y.H. (2023). Four years field measurements in a partly submerged woven geotextile-reinforced pile-supported embankments. *Geosynthetics: Leading the Way to a Resilient Planet. Proc. 12ICG,* 1072-1077.

van Eekelen, S.J.M., Wittekoek, W., Zwaan, R.A., Bezuijen, A., Nancey, A. (2024). Groundwater in geosynthetics-reinforced pile-supported embankments, 3D experiments. *Proc. ECSMGE 2024.* Lisbon, Portugal.

Wang, H.L, Chen, R.P., Cheng, W., Qi, S., Cui, Y.J. (2018). Full-scale model study on variations of soil stress in geosynthetic-reinforced pile-supported track bed with water level change and cyclic loading. *Can. Geotech. J.* 56: 60–68 (2019) dx.doi.org/10.1139/cgj-2017-0689.